Astron. Astrophys. 319, 607–616 (1997)

ASTRONOMY
AND
ASTROPHYSICS

SiO high velocity maser emission in O-rich evolved stars

J. Cernicharo[1], **J. Alcolea**[1], **A. Baudry**[2], **E. González-Alfonso**[1,3]

[1] Observatorio Astronómico Nacional, Apartado 1143, E-28800 Alcalá de Henares, Spain
[2] Observatoire de Bordeaux. B.P. 89, F-33270 Floirac, France
[3] Universidad de Alcalá de Henares, Departamento de Física, Campus Universitario, Alcalá de Henares, E-28871 Madrid, Spain

Received 14 February 1996 / Accepted 9 August 1996

Abstract. Highly sensitive simultaneous observations of the 2→1 line of the first vibrationally excited state of SiO, and of the 2→1 line of CO have been obtained toward 37 O-rich evolved stars. In $\sim$ 45% of these objects, the SiO line profiles present unusually broad wings, reaching, and in some cases exceeding, the terminal velocity of the circumstellar envelope. All of the objects exhibiting SiO line wings are Mira or semiregular variables and most of them have terminal velocities for their circumstellar envelopes below 10-12 kms^{-1} and moderate mass loss rates. In the opposite, all the OH/IR stars have very narrow SiO lines relative to the CO linewidth.

In R Leo, the velocity extent of the SiO emission shows a time variability. Variations of the SiO line wings are also observed in other O-rich stars between 1994 and 1995. The time variations observed in these objects suggest changes in the physical structure and velocity field of the innermost regions of the envelopes over timescales of months/years no necessarily related to the periodic optical pulsation of Mira stars.

Our data, which lack of angular resolution to resolve the SiO emission, cannot give an unique answer to the origin of the SiO line wings. However, radiative transfer models indicate that in stars with large terminal velocities for their circumstellar envelopes, the effects of turbulence and rotation are negligible in the emergent line wings. On the contrary, rotating Kleperian disks can produce prominent line wings in envelopes with moderate or low terminal velocities. The effect of asymmetric mass loss processes and of gas infall/outflow on the emergent SiO line profile have been also analyzed and can explain, at least qualitatively, the presence of SiO line wings.

Key words: circumstellar matter – stars: AGB, post-AGB – radio lines: stars – Masers – lines: profiles

1. Introduction

SiO maser emission can be used to investigate the physical conditions in the innermost layers of the circumstellar shells around oxygen-rich late-type stars (see, e.g., Cernicharo et al. 1994 or the review by Baudry 1993). These regions are hidden in the thermal emission of molecular lines, while the maser nature of the SiO v=1 emission allows us to probe some characteristics of the immediate photospheric environment. Recently, Cernicharo et al. (1994) observed in R Leo a v=1, J=2→1 SiO emission at velocities larger than the terminal velocity (V_t) of the expanding circumstellar CO gas. Cernicharo et al. also made lunar occultation observations of the SiO maser emission in this object founding (i) a rather compact rotating structure corresponding to the bulk of the SiO line profile; and (ii) two extended lobes, or opposite regions in the plane of the sky, associated with the blue and red wing SiO emission near the terminal velocity of the circumstellar envelope. On the other hand, recent VLBI observations of the v=1, J=1→0 line of SiO have been made in the late-type stars U Her, TX Cam, W Hya, and VX Sgr (Diamond et al. 1994; Miyoshi et al. 1994; Greenhill et al. 1995). The SiO emission in the three first objects can be explained as arising from shell/ring-like structures. VX Sgr shows, however, an asymmetric distribution of the SiO emission which leads Greenhill et al. to suggest the existence of an asymmetry in the mass-loss or in the stellar atmosphere. The comparison of the regions where the SiO and the circumstellar dust emission arise indicates that the former originates between the star photosphere and the outer edge of the shell where dust is formed.

Although single-dish telescope observations of SiO maser emission lack the angular resolution of VLBI, they offer a sensitivity large enough to reveal details of the emission at high velocities, and hence of the velocity field in the innermost layers of the circumstellar envelope. These regions are of particular interest as dust is formed there and the velocity field is a tracer of the dynamical processes occurring in the region prior to the acceleration of the molecular envelope. In this paper we present sensitive observations of the v=1 J=2-1 SiO maser emission toward 37 O-rich evolved stars, together with the thermal emission of the J=2→1 line of CO. The objects have been selected to cover a large variety of long period variables, including Miras, semiregulars, supergiants, and OH/IR stars. They are listed in Table 1.

Send offprint requests to: J. Cernicharo

Table 1. Stellar sample and observed line parameters for January 1994 observations

Stars	Stellar Class	CO J = 2-1 σ mK	T_{MB} K	V_{LSR} kms^{-1}	Δv(2σ) kms^{-1}	$\int T_{MB} dv$ K kms^{-1}	SiO v = 1 J = 2-1 σ mK	T_{MB} K	V_{LSR} kms^{-1}	Δv(2σ) kms^{-1}	$\int T_{MB} dv$ K kms^{-1}	R	Comments
a - Miras and Semi-Regulars													
Y Cas	Mira	40	0.42	-16.9	23.6	8.5	47	6.2	-17.6	14.8	32.6	0.63	R
T Cas	Mira	50	0.67	-6.3	20.0	11.7	94	6.6	-5.9	11.1	21.4	0.56	
R And	Mira	41	2.40	-15.5	21.8	35.4	43	4.4	-17.1	20.1	20.1	0.93	R
IRC+10011	Mira	66	4.00	9.6	39.3	117.5	51	19.5	6.6	11.8	60.3	0.30	
o Ceti	Mira	61	18.1	46.2	18.7	84.0	52	18.5	46.2	8.2	34.7	0.44	
S Per	SRc	60	0.26	-36.6	35.9	8.7	43	10.3	-41.7	34.0	117.3	0.95	* B
NML Tau	Mira	50	4.95	35.0	40.8	171.4	46	89.6	34.0	16.8	358.7	0.41	
TX Cam	Mira	120	4.94	11.8	40.8	150.5	102	15.6	9.8	13.2	73.4	0.32	
U Ori	Mira	34	1.17	-38.5	16.9	12.6	36	72.1	-40.9	18.6	213.1	1.10	RB
V Cam	Mira	58	0.53	8.3	31.1	14.5	120	21.0	7.0	15.4	57.2	0.50	
GX Mon	Mira	59	3.05	-9 .0	39.2	92.7	118	12.2	-8.5	11.1	57.6	0.28	
VY CMa	Mira	85	1.78	21.1	95.0	121.7	69	346.	22.9	49.7	3001.	0.52	#
S CMi	Mira	62	0.70	51.5	7.2	3.1	57	2.7	50.3	9.6	12.7	1.33	R
W Cnc	Mira	48	0.50	36.0	15.7	6.0	45	7.3	38.3	14.4	25.4	0.92	R
R LMi	Mira	37	1.02	0.2	19.5	13.8	32	15.0	-1.1	13.6	52.1	0.70	R
R Leo	Mira	43	1.54	-0.5	15.7	18.9	66	117.	-2.4	15.7	320.9	1.00	RB
R Crt	Mira	87	2.50	11.4	23.5	51.0	50	6.8	7.0	19.3	51.0	0.82	B
RT Vir	SRb	38	2.11	17.5	18.8	30.4	26	14.6	15.3	22.9	71.7	1.22	RB
SW Vir	SRb	102	1.52	-11.0	14.9	20.4	173	1.6	-12.6	8.2	8.3	0.55	R ?
R Hya	Mira	140	2.09	-10.8	15.9	23.6	41	24.3	-10.3	8.5	50.1	0.53	
W Hya	SRa	61	1.53	40.4	17.2	22.0	65	225.	40.1	22.4	683.5	1.30	RB
RX Boo	SRb	62	3.11	1.6	19.5	51.8	44	7.9	-1.5	12.6	35.1	0.65	
S CrB	Mira	56	1.13	1.1	15.0	12.1	39	35.4	0.8	14.2	105.5	0.95	
RU Her	Mira	63	0.65	-12.2	16.4	9.5	51	6.2	-13.2	13.9	22.7	0.85	R
U Her	Mira	59	0.65	-15.0	19.9	10.3	51	16.3	-17.6	14.7	57.2	0.74	
VX Sgr	SRc	84	1.50	8.1	47.8	66.8	80	52.7	6.3	38.4	622.5	0.80	*
R Aql	Mira	87	3.37	47.3	18.8	49.2	62	13.1	47.2	11.6	33.2	0.62	
T Cep	Mira	45	1.66	-3.3	11.8	13.4	86	24.7	-0.5	12.6	93.0	1.07	RB
μ Cep	SRc	35	0.15	24.8	35.9	5.1	35	25.9	25.6	65.7	142.4	1.83	* RB
R Cas	Mira	72	4.35	25.5	28.8	86.8	61	60.0	25.3	19.1	281.3	0.66	
b - OH-IR and Infared Objects													
IRC+30021		76	1.01	-26.8	28.0	22.1	82	4.0	-28.0	9.9	12.7	0.35	M
OH127.8-0.0		60	0.55	-54.5	22.7	9.9	64	0.4	-56.0	4.7	1.7	0.21	*
IRC+60154		60	0.63	51.7	31.0	16.7	88	12.6	48.7	14.6	44.2	0.47	M
IRC+70066		130	1.56	-1.3	37.7	51.8	104	8.5	-1.1	11.1	28.0	0.29	M
OH63.3-10.2		42	0.42	-71.8	33.4	11.6	67	3.6	-72.5	7.3	8.1	0.22	
NML Cyg	Irreg	62	4.12	0.2	69.9	220.8	52	12.9	-12.6	49.2	116.3	0.70	# M
OH104.9+2.4		42	0.28	-25.8	33.6	8.4	77	0.5	-28.4	6.0	1.6	0.18	

Notes :

(*) CO line contaminated by galactic emission

(#) CO line shows a red and/or blue wing

(R) the SiO red wing reaches or surpasses the most positive CO velocity

(B) the SiO blue wing reaches or surpasses the most negative CO velocity

(M) late M spectral classification

2. Observations

The observations were carried out with the 30 m IRAM telescope on 14 January 1994 and June 1995. Most of the data present here were taken during the first run. Two SIS receivers were simultaneously used at 86 and 230 GHz. During this run, the sky was clear, the ambient temperature was close to –10°C and the relative humidity was nearly zero; consequently, the transmission at these two frequencies was excellent (a zenith opacity lower than 0.04 was measured at 230 GHz during the observations). The 3mm receiver was tuned in SSB mode at the frequency of the v=1 J=2→1 line of SiO; the attenuation of the image band being about 10 dB. The SSB receiver and system temperatures were 80 and 140 K respectively. The 1mm receiver

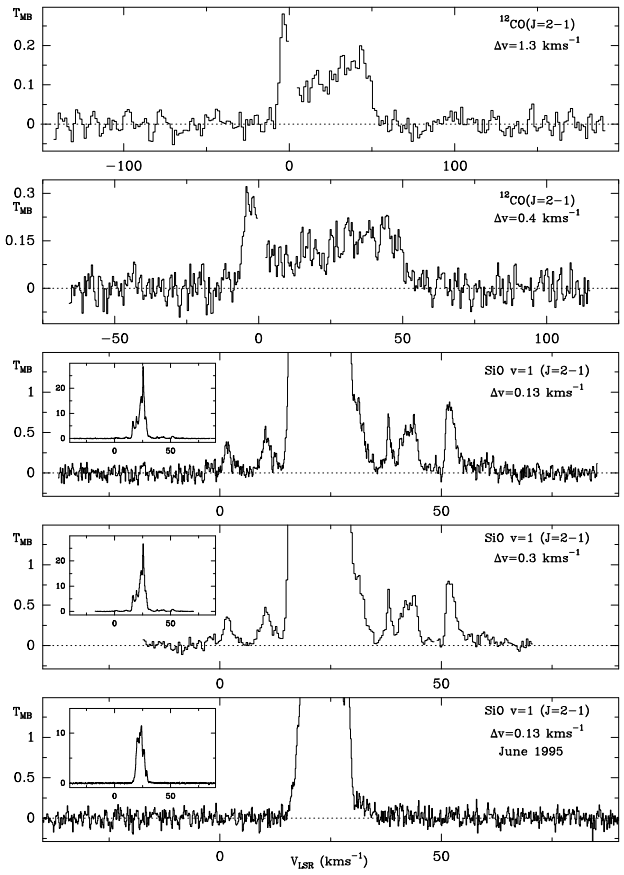

Fig. 1. CO J=2→1 and SiO v=1 J=2→1 emission toward μ Cep. All the spectra have been obtained in January 1994 except the bottom one which was taken in June 1995. From top to bottom the backends are : 1 MHz filterbank, autocorrelator with $\Delta\nu$=320 kHz, autocorrelator with $\Delta\nu$=40 kHz, 100 kHz filterbank and autocorrelator with $\Delta\nu$=40 kHz. All the observations were obtained with the wobbling system. A degree 1 baseline has been removed for each spectrum. Note the important change in the SiO line profile between 1994 and 1995.

was tuned, also in SSB mode, at the frequency of the J=2→1 line of CO, the SSB receiver and system temperatures being 100 and 180 K respectively. The main beam telescope efficiencies at the frequencies of the CO J=2-1 and SiO v=1 J=2-1 lines are 0.45 and 0.60 respectively (main beam brightness temperature for SiO can be translated into flux in Jy by multiplying the corresponding intensities by a factor 4.5).

The pointing was frequently checked by observing the SiO maser line itself using 16 channels of the 100 kHz filterbank. Both the absolute pointing of the 3mm receiver, and the alignment between the two receivers were better than 2″. The focus adjustment was also checked every hour in the same pseudo-continuum mode.

The spectrometers consisted of two 512×1 MHz filterbanks, a 2048-channel autocorrelator, and a 256×100 kHz filterbank. In SiO the spectral resolution was 3.6 km s^{-1} for the 1 MHz filters, and 0.07 km s^{-1} for the correlator. In CO it was 1.3 and 0.05 km s^{-1}, respectively. For all stars, the autocorrelator spectra for SiO, when smoothed to 0.35 km s^{-1}, were similar to that produced by the 100 kHz filterbank. (i.e., no artificial broadening of the lines was observed in the autocorrelator). Due to the large intensity of the SiO maser emission, weak spurious features could appear after heterodyne mixing. In order to suppress such possible features, the sideband noise level of the phase-lock loop signal was adjusted to less than –40 dB. All observations were performed with the wobbling system with the OFF reference position 120″ away in azimuth from the source and with a wobbling time phase of 2 seconds. This observing procedure provides excellent baselines for spectral data. Line calibration was achieved using two absorbers at different temperatures and by observing the sky emissivity to derive atmospherical opacities. Fig. 1 shows a few SiO and CO spectra observed toward μ Cep taken with different spectrometers (a degree 1 baseline has been removed). The quality of the baseline allows a good comparison of the CO and SiO line wings in each observing run.

For the June 1995 run the observing procedure and instrumental configuration were similar to those of 1994 except for the pointing which was done on strong continuum sources. Hence, pointing accuracy in this second run was slightly poorer and around 4″.

3. Results

In Table 1 we list the observed sources and the corresponding CO and SiO line parameters. In subtable a we gather the Mira and optical semiregular variables and in subtable b we present the OH-IR stars and other infrared objects. For SiO, the main beam brightness temperature and velocity correspond to the strongest feature. For CO, the main beam brightness temperature corresponds to the intensity averaged over a few channels around the line center; the corresponding velocity is the line profile centroid. For each line, the full velocity coverage above 2σ has been determined and the corresponding values are given in Table 1. The SiO and CO lines have been observed with different backends at different spectral resolutions. Consequently, it was easy to check that the observed SiO line wings were real and not an artifact in one of the spectrometers. In addition, when the SiO line wings were particularly prominent the observation was repeated after the sideband noise level of the phase-lock loop-gain was checked and ajusted to the minimum aceptable value (–40 dB). Figs. 2 and 3 show the line profiles, smoothed to 0.4 km s^{-1} for both molecules, in selected objects showing weak red and/or blue SiO emission. Fig. 4 shows the observed CO and SiO line profiles in the remaining objects. Fig. 5 shows a comparison of the SiO spectra for the stars observed in both periods.

In Table 1, the SiO velocity peak agrees for most of the objects with the CO velocity centroid which is a good estimate of the systemic stellar velocity (see also Jewell et al. 1991); this suggests that the bulk of the maser amplification occurs in the immediate neighbourhood of the star, where the gas has not yet been fully accelerated, or that the velocity vectors are perpendicular to the paths of maximum amplification. In addition, all

strong peaks with narrow SiO emission lie inside, and spread over, the full velocity range of the thermal CO emission. Presumably, the line wings of v=1 SiO emission are of maser nature, as no trace of high velocity gas emission has been observed in thermal v=0 SiO emission (see Fig. 4 in Cernicharo et al. 1994). Moreover, a full track in parallactic angle of R Leo with the 30 m IRAM telescope (unpublished data) has revealed that its SiO v=1 J=2→1 line wings are strongly linearly polarized.

Because most stars in our sample have high galactic latitudes, the blending of CO stellar lines with interstellar CO is not a major problem. However, in those stars with low galactic latitudes, contamination by interstellar cloud emission may be present. Such an emission is narrow compared to the broad stellar CO profile and, when present, may fall outside (e.g. S Per, see Fig. 2) or within the stellar profile (e.g. VX Sgr, TX Cam, OH104.9+2.4, OH127.8-0.0 in Fig. 4). The coincidence with the edge of the stellar CO profile perturbs the CO widths analysis in the case of μ Cep (see Figs. 1 and 2). This object shows galactic contamination in the blue part of the CO profile; from the shape of the profile we have adopted a CO velocity range between 0 and 50 km s^{-1} (between 14 and 50 km s^{-1} above 2σ); in any case, due to this problem this object will not be considered in the discussion.

In order to find out whether the SiO emission range is broader than that of the CO emission, we derive the SiO and CO line widths to 2σ intensity and compute the ratio R=Δv(SiO)/Δv(CO). This ratio is given in column 12 of Table 1, and varies between 0.18 for OH104.9+2.4, and $\sim$ 1.83 for μ Cep (however, see comments above for this object). The average R value for Miras (Table 1a) is 0.7. 52% of these objects have $R \geq 0.7$ and tend to show prominent red wings (see comments in Table 1 and Discussion), and 17% (four Miras) have $R \geq 1$ (see Figs. 2 and 3). We will consider that an object shows high velocity wings when it displays red and/or blue wings which can occur independently of value of R. All the objects with $R \geq 1$ have SiO wings exceeding the CO emission both in the blue and in the red with the exception of S CMi where only the SiO red wing surpasses the CO terminal velocity. The three supergiants in subtable a have R in the range 0.8 to 1.8 and the four semiregular variables have R between 0.6 and 1.3. The infrared objects in subtable b have an average R value of 0.29 when one excludes the irregular supergiant NML Cyg.

Stars with SiO velocities more negative than in CO are not easily interpreted due to trapping of CO blue photons in the outer layers of the circumstellar envelope (which leads to a self-absorption in the blue part of the CO profile, see e.g. Huggins & Healy 1986). Hence, the measured CO velocity extent toward the blue must be considered a lower limit. Therefore, for stars with blue SiO wings, we can only conclude that SiO emission reaches or approaches the terminal velocity of the envelope. In the red part of the CO line profile it is difficult to produce self-absorbed effects similar to those mentioned above, unless we invoke non-standard velocity fields. For R larger than 0.7 most of the stars show SiO line velocities exceeding the CO velocities in the red, and hence this SiO emission represents a gas component that is not detected in the thermal emission of CO and other molecular species.

A plot of the ratio R versus the mass loss rates deduced from CO observations (Loup et al. 1993) shows that large values of R tend to be found in stars with low mass loss rates. This is also true when one plots R versus the the IRAS 25 to 12 μm flux ratio which is also a measure of the dust mass loss rate (Loup et al. 1993; however, this trend may need to be corrected for a possible dependence of R on the optical light phase; see below). The bulk of our sample lies in regions II and IIIa of the two-colour plot by van der Veen & Habing (1988). Stars with $R \geq 1$ do not show any particular behaviour in this plot and all lie near the Mira evolutionary track. It is worth noting that stars with $R \geq 0.7$ are Mira or semiregular variables, whereas those with the lowest values of R are OH-IR stars. Finally, all stars in our sample showing blue and/or red wings (independently of the value of R) are characterized by moderate values for the terminal velocity of the envelope, $V_t \leq$10-12 km s^{-1}, except S Per and μ Cep (both have $V_t \sim$ 17.5 kms^{-1} and both are known to be supergiants).

A previous comparison between SiO and CO line profiles has been done by Nyman & Olofsson (1986), but due to limited signal to noise ratio they compared the long term averaged profile of SiO with CO expansion velocities. They concluded that the SiO velocity coverage could be larger than the CO velocity extent for R Leo, U Ori and o-Cet. However, the CO expansion velocities in their Table 3 are clearly underestimated when compared with our CO data (see our Table 1). For instance, for R Leo and o-Cet they found a CO velocity coverage of 12 and 9.8 kms^{-1} while in our data it is of 15.7 and 18.7 km s^{-1}respectively (see Table 1). With our CO data the R values of Nyman & Olofsson for these stars are smaller than 1.

4. Variability

Experience shows that the CO velocity coverage does not change with time, therefore any change in the ratio R means a change in the SiO line, presumably due to stellar activity.

If the SiO line wings are related to the stellar pulsation activity of Mira stars, one could expect a variation of R with the stellar phase. R Leo is perhaps the most representative case showing extreme SiO wing variations. Cernicharo et al (1994) reported broad red and blue wings (R=1.90) and discrete maser features at large red velocities in different SiO maser lines. We have monitored the SiO v=1 J=2→1 maser emission from this star with the IRAM interferometer (unpublished data). Gathering the interferometer and 30 m data, R varies from 0.96 in April 1991 to 1.53, 1.90, 0.83, 0.86, 0.67, 1.0, 1.08 and 1.0 in June 1992, November 1992, January 1993, May 1993, November 1993, January 1994, May 1994, and June 1995 respectively (the light phase being 0.3, 0.7, 0.2, 0.4, 0.8, 0.4, 0.6, 0.0, and 0.6 respectively).

In 1995 we have reobserved a few objects. The SiO profiles are shown in Fig. 5, together with those obtained in 1994 for SiO and CO. The line profile in all these objects shows an important variation between both periods. The more remarkable cases are

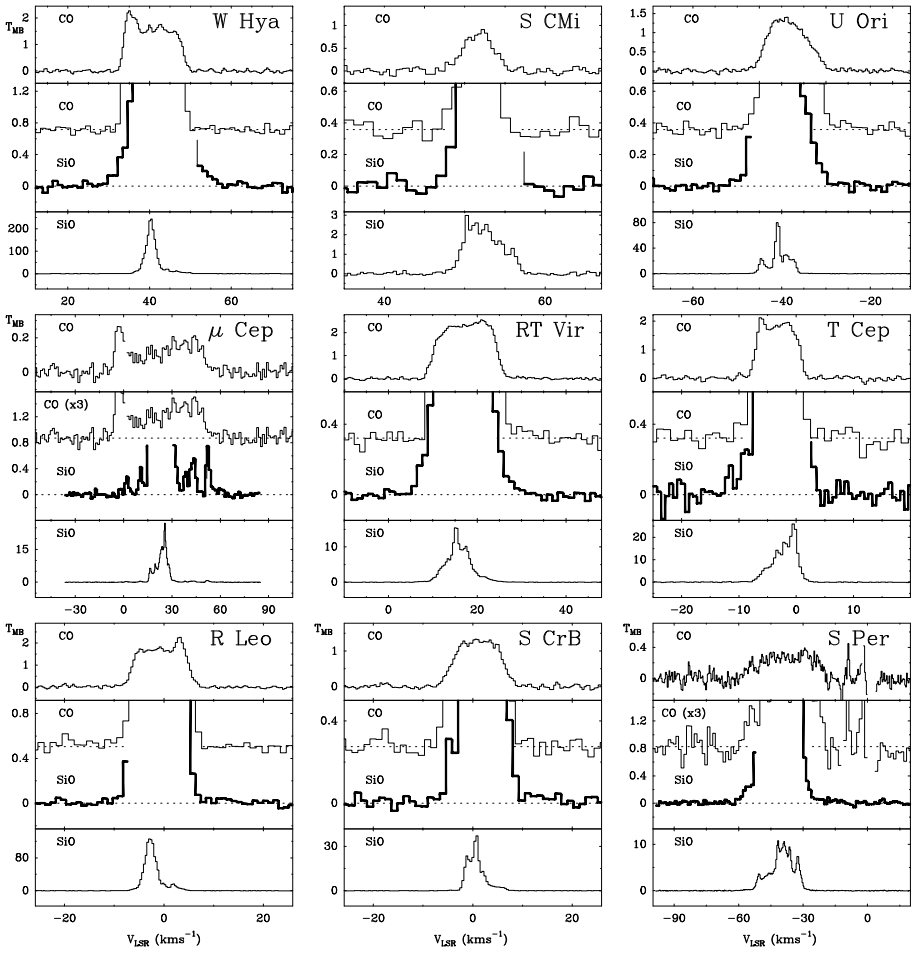

Fig. 2. CO J=2→1 and SiO v=1 J=2→1 line profiles toward selected objects from Table 1 with $R \geq 0.95$ (see Table 1). The intensity scale is in main beam brightness temperature and the velocity is relative to the LSR. For each object the CO and SiO full profiles are given in the top and bottom panels, respectively. The center panel shows an enlargement of the CO (thin line) and SiO (thick line) profiles. For μ Cep the CO blue profile is contaminated by galactic molecular cloud emission. The SiO profiles in the center panels are clipped when intersecting the CO ones. Zero level emission for both CO and SiO lines in the center panel are marked with horizontal dashed lines. Original spectra in this panel have been smoothed by adding two or three adjacent channels to improve the signal to noise ratio in the line wings.

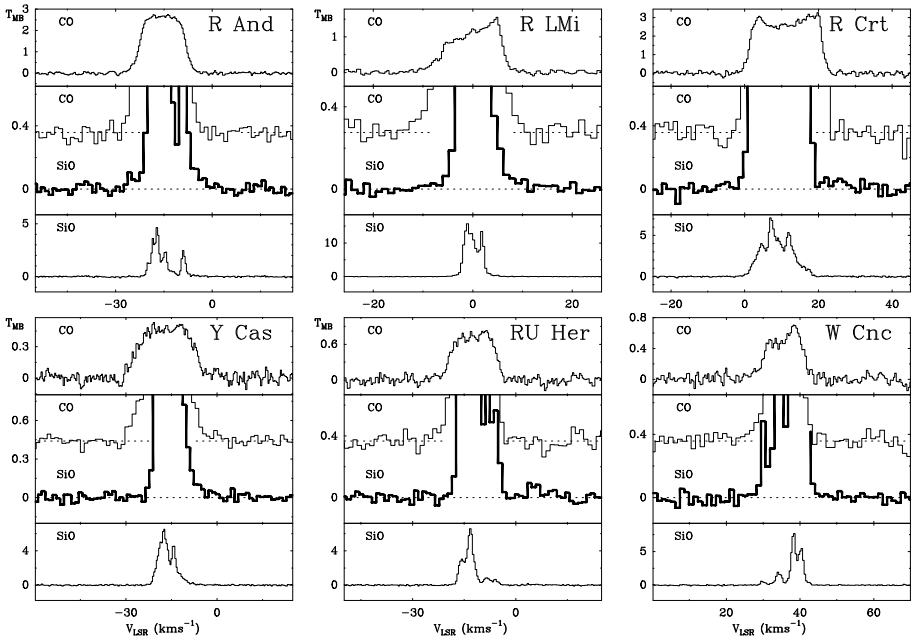

Fig. 3. Same as in Fig. 2, but for stars with $R \leq 0.95$ (see Table 1).

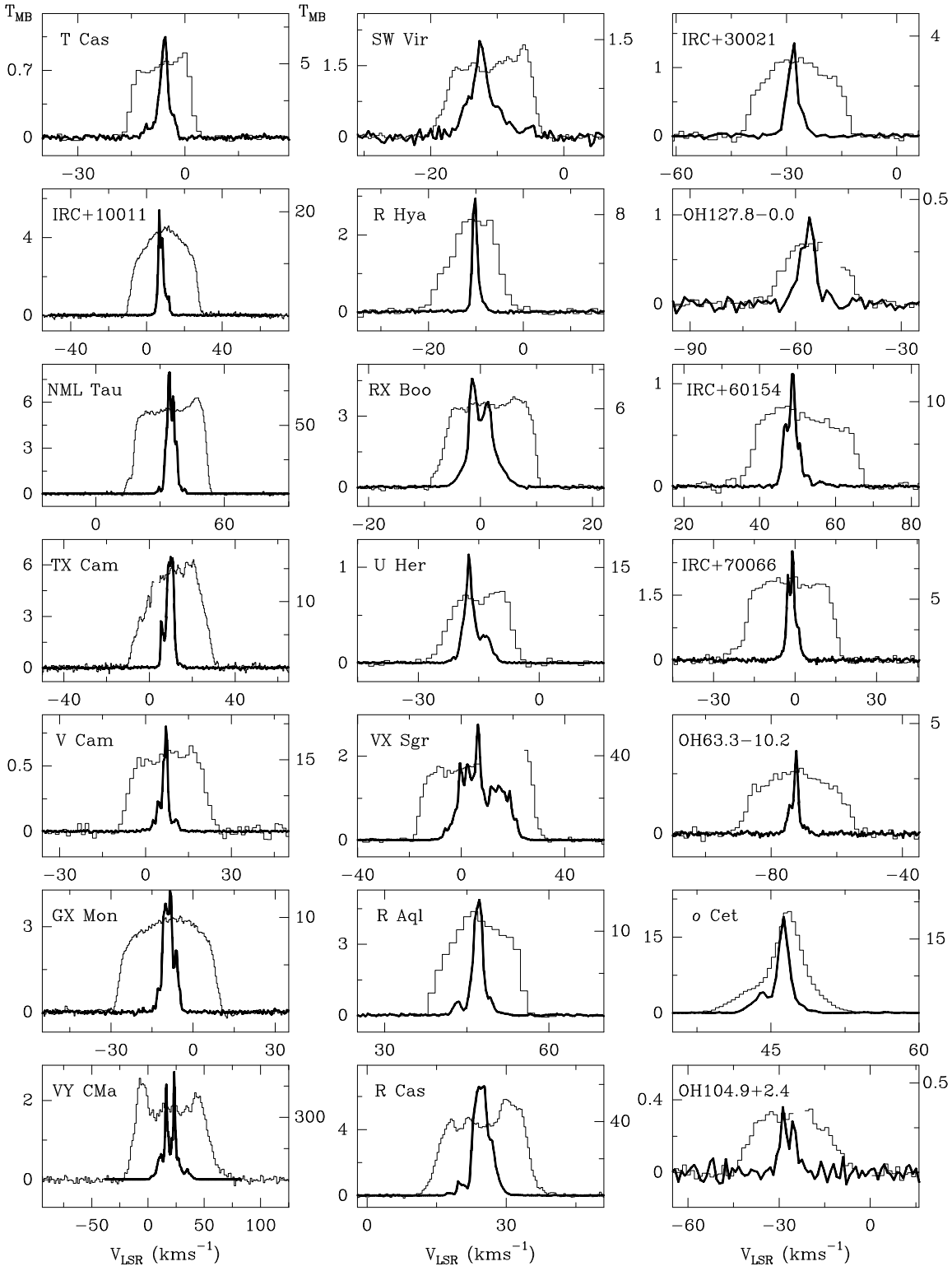

Fig. 4. CO $J = 2 \rightarrow 1$ (histogram plot) and SiO v=1 $J = 2 \rightarrow 1$ (thick continuous line) spectra for stars of Table 1 with $R \leq 0.7$. The left and right Y-scales correspond to CO and SiO intensities respectively. For both lines the intensity scale is in main beam brightness temperature. Some stars are contaminated by galactic CO emission (TX Cam, VX Sgr, R Aql -mainly outside the line core-, OH104.9+2.4, and OH127.8-0.0); the corresponding channels have been omitted in the plots.

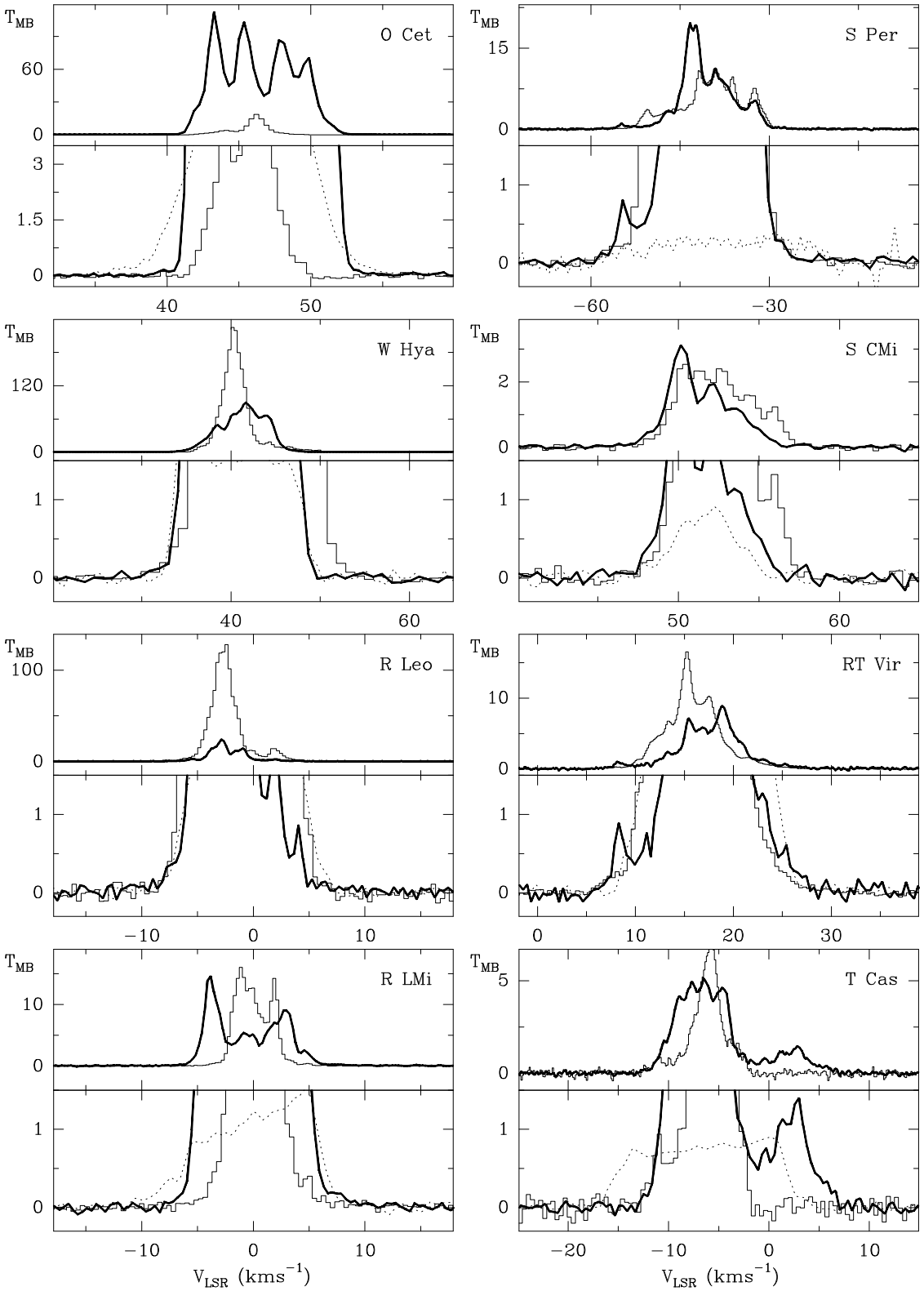

Fig. 5. Comparison of the SiO emission in 1994 (histogram plots) and 1995 (thick continuous line) for some objects observed in both periods. For each star the top panel shows the full main beam brightness temperature scale and the bottom panel corresponds to an enlargement of the same data. The bottom panel for each star also shows the CO $J = 2 \rightarrow 1$ spectrum (dashed line).

o Cet, T Cas, R LMi, and W Hya. o Cet is known to have a bipolar structure for the distribution of the CO emission (Planesas et al, 1990; Planesas, Kenney and Bachiller 1990). In our SiO spectrum of 1995 the emission reaches the red edge of the CO profile and approaches the blue one. However, in 1994 the SiO emission was narrower and concentrated toward the central velocities. Our 1995 spectrum is much similar to that observed by Wright et al. in 1990. The value of R changes from 0.44 in 1994 (see Table 1) to 0.85 in 1995 (stellar phase = 0.6 and 0.2 respectively). Moreover, the 1995 spectrum shows prominent blue and red wings that were not present in 1994. These wings are not discrete features but form a continuous and strong broad pedestal (see Fig. 5 top panel). The H_2O VLA map of this source by Bowers and Johnston (1994) shows a line with a width at half power of 2 kms^{-1} and a spatial distribution indicating an elongated structure in the NE-SW direction. Other observations in the optical and infrared also indicate an asymmetric structure near the star (Karovska et al 1991, Haniff et al 1992; Danchi et al 1994). These observations could suggest that asymmetric mass loss processes may play a role in the formation of blue and red wings maser emission in SiO.

T Cas shows impressive changes in the SiO profile. In the 1995 observations the line profile exhibits several features in the red part of the CO line. The strongest feature is centered at the terminal velocity and exceeds the CO line by roughly 5 $\mathrm{km\,s}^{-1}$. The value of R changes from 0.56 to 1 between both observing periods (stellar phase = 0.9 and 0.0 respectively). In the blue part, the velocity extent looks similar in 1994 and 1995; however, in the latter observations the blue SiO emission is stronger (see bottom-right panel of Fig 5).

R LMi shows in 1995 a double peaked profile with a weak feature near the central velocity of the star. The SiO line profile reaches and exceeds the CO profile in the red. The R value in 1995 is $\sim$ 0.9 (stellar phase = 0.8) while in 1994 it was 0.7 (stellar phase = 0.4).

Contrary to other stars, the SiO line profile in W Hya is narrower in 1995 than in 1994. Nevertheless, R is $\sim$ 1 in 1995 (see Fig. 5). In 1994 this value was 1.3 (see Table 1). The correspondig stellar phases were 0.8 and 0.1 for 1994 and 1995 observations.

Finally, the most impressive change in the SiO line profile was observed in the supergiant μ Cep (see Fig 1). All of the high velocity discrete features detected in 1994 disappeared in 1995. Although the CO line profile is blended with interstellar emission and R is poorly determined, R changes by a factor $\sim$ 2 between both observing runs.

The broad wings reported by Cernicharo et al (1994) in R Leo for SiO v=1 J=2$\rightarrow$1 and the discrete features at high velocities for other high v transitions of SiO have been only observed in 1992. Some of the additional observations for the same star are at similar light phases but only moderate wings have been observed. It is worth noting that during the 1992 observations of R Leo, the SiO maser emission had a particular strong maximum (Alcolea et al, in preparation). In other stars we find that R increases after the optical maximum (o Cet, T Cas, R LMi) while in W Hya the situation is the opposite. These results could suggest that in some objects (e.g. R Leo, W Hya) there are changes in spatial structure and velocity field over a timescale of a few months/years not related to the periodic optical pulsation of Mira stars. Observations of H_2O in W Hya by Reid and Menten (1990) and Bowers and Johnston (1994) also indicate similar results (note that this object shows a prominent red wing in Fig. 2; this wing disappeared in 1995 -see Fig. 5). Although our limited data do not indicate correlation between R and the stellar phase, a more detailed monitoring study of the SiO emission is necessary to determine the effect of stellar phase on the emergent SiO profiles. All other Miras with $R \geq$ 1 had a light phase in January 1994 between 0.5 and 1.0.

5. Discussion

In the analysis of the SiO line wings two possibilities could be considered : a) the region where SiO line wings are formed coincides with the zone where the terminal velocity of the circumstellar envelope has been reached and, b) the SiO line wings are formed in the innermost regions of the envelope where the radial velocity associated to the expansion of the envelope is still small, but where the kinematics of gas allows velocities larger than V_t. In both cases different kinematical processes could contribute to the production of SiO line wings such as : (i) turbulent motions; (ii) rotation ; (iii) gas infall and outflow; and (iv) asymmetric mass outflow. We will analyze now the possibility to produce weak SiO maser emission at velocities similar or larger than V_t for these different cases.

5.1. Turbulent motions

The simplest models for circumstellar envelopes suggest a spherical envelope expanding with a constant radial velocity, V_t, for distances larger than a few stellar radii. Between the stellar photosphere and the outer circumstellar layers the gas is accelerated, and its velocity increases monotonically until it reaches V_t (see, e.g., Kwok 1975; Goldreich and Scoville 1976). In order to study qualitatively the conditions for which SiO v=1 J=2$\rightarrow$1 line wings may form under the assumption of monotically increasing radial velocity fields, we have modelled the SiO emission by means of a non-local radiative transfer code that has been described in detail by González-Alfonso (1995) and González-Alfonso & Cernicharo, (1996, in preparation).

Our calculations indicate that a combination of high mass loss rate, low terminal velocity and large turbulent motions can produce weak blue wings reaching the terminal velocity of the envelope. However, our models fail to produce redshifted wings. Turbulence would apply to some stars showing blue wings, narrow linewidths, and high mass loss rates. If the regions where the line wings arise are very close to the star, the shadowing of the gas behind the central object could be important. In this case, our models predict mainly blue wings. However, only S Per and R Crt show a blue wing without red counterpart. Our observations (see Table 1) indicate that in most cases the SiO wings appear in the red. Hence, the standard kinematical mod-

els even in the presence of high turbulence seem insufficient to explain the full behaviour of the SiO maser wing emission.

5.2. Rotation

Rotation has been invoked by van Blerkom and Auer (1976), van Blerkom (1978), and Zhou Zhen-pu and Kaifu (1984) to explain the SiO J=1→0 v=1, 2 line profile in VY CMa.

Rotational velocities in a kleperian disk can be large near the central star and can play a role in the formation of the of the SiO line wings. However, the dependence of the angular velocity versus radius as $r^{-3/2}$ reduces considerably the effect of rotation on the SiO line wing profile for longer distances. For instance, for a star with a mass of 1 $M_\odot$ and a radius, R_s, of 5 10^{13} cm, the keplerian rotational velocity, V_{rot}, is $\sim$ 16 km s^{-1}at r=2 R_s, but reduces to $\sim$ 8 km s^{-1}at r=8 R_s. If strong amplification occurs near the star as VLBI and lunar occultation data seem to indicate, and if V_t is similar or smaller than V_{rot} at r=2-3 R_s, the effect of rotation in the formation of line wings exceding the terminal velocity must be considered for envelopes with moderate or low expansion velocities, $\lesssim$ 15 km s^{-1}.

As mentioned above, all stars showing high values of R have moderate terminal velocities, $V_t \sim$ 10-12 km s^{-1}. The question that now arises is whether maser amplification near the star can take place under this geometry and kinematics. To elucitade this question and in order to evaluate qualitatively the effect of rotation in the formation of line wings we have modelled the SiO maser emission in a kleperian rotating non-expanding ring, using a non-local radiative transfer code (González-Alfonso 1995; González-Alfonso & Cernicharo, in preparation). The results show that the v=1 J=2–1 line is inverted (by the stellar radiation) only in the innermost part of the ring, where the rotation velocity is the highest (11 km s^{-1}). In other regions the inversion disappears beacuse the opacity in the axial direction becomes smaller than that in the radial direction. The emergent profiles consist then of two pronunced peaks at the extreme (rotation) velocities, $\pm$ 11 km s^{-1}. The predicted two peaked structure is not seen in the profiles, but note that the real kinematics in the inner envelope must be much more complex than the simple model used here. We conclude that rotation can not be eliminated as possible candidate for the origin of (some of) the line wings we have detected in SiO.

5.3. Pulsation: gas infall

For Mira and semi-regular variable stars, pulsation models indicate a complex velocity field near the star with successive gas infall and outflow. The gas also reaches the terminal velocity but, in the innermost part of the envelope the gas velocity can be larger than V_t (Bowen 1988). The presence of infalling and outflowing gas layers due to the stellar pulsation could produce red and blue features from the gas lying in front of and/or behind the star. The later part could contribute to the emission provided that shadowing by the star is not important. If shadowing is important, however, red wings may still arise from the infalling gas in front of the star. In this context, the broad SiO line wings could be related to the optical or infrared absorption lines observed in the same kind of objects (e.g. Barbier et al. 1988; Hinkle 1978). However, the lack of general trend between R and the stellar phase for all observed stars indicates that more complex processes must be invoked to explain the data.

5.4. Asymmetric mass loss

Asymmetric mass loss processes could also constitute a natural explanation for the observed SiO line profiles. The only high angular resolution observations of the weak and broad SiO wings available in the literature are the lunar occultation data for R Leo reported by Cernicharo et al. (1994). These observations show that the line wings are detected far from the star ($\sim$4–5 R_*), and are probably produced by an asymmetric mass loss process. High resolution studies from VLA observations of OH and H_2O (see Bowers, Johnston and Vegt 1989 and Gómez et al 1994) also indicate that outflows from evolved stars are not isotropic but axisymmetric. In U Ori, Bowers & Johnston (1988) propose a model for the maser region in which OH is distributed in axisymmetric, biconical density concentrations embedded in an approximately spherical shell. Bowers, Johnston and de Vegt (1989) also propose for NML Tau, U Her, R Aql, RR Aql, and S Per similar axisymmetric structures in the expanding shells, with the shell of RR Aql being highly asymmetric. For their data they exclude radial acceleration, rotation or random velocity fields as origin of the distribution of OH and H_2O masers and propose outflow of gas in a radially expanding ellipsoidal configuration with gas density being a function of radial distance and latitude from the equatorial plane of the star. In particular, they found that U Her and U Ori show blue and red features separated into opposite quadrants on the sky, a result similar to that found by Cernicharo et al (1994) for the SiO line wings emission in R Leo. All the objects quoted above also present red or blue SiO wings in our data.

The relatively large number of stars showing SiO broad wings (this work) and H_2O velocity anomalies (Gómez et al, 1994), could also be related to the presence of binary systems (Morris 1987, 1990). The complex kinematic effects related to binary- or multiple-star systems may mean that asymmetric or axisymmetric mass loss processes are common in evolved O-rich stars. In this context, o Cet, a known binary sistem with a slow bipolar outflow, shows in our 1995 observations a broad pedestal in SiO emission which practically covers, at least in the red part of the spectrum, the outflow velocities as traced by the emission of CO. The case of o Cet suggests that bipolar mass loss processes could also play a role in the formation of SiO line wings.

6. Conclusions

We have observed a sample of 37 O-rich stars (30 Miras and semiregular variables, and 7 OH-IR objects) with the 30-m IRAM radiotelescope in the lines of SiO v=1 J=2→1 and ^{12}CO J=2→1. Broad SiO wings have been detected in 52% of the Mira and semiregular stars. Most of these wings appear in the

red part of the line reaching and even exceeding the corresponding CO velocities. A few objects show broad wings in the blue and in the red.

The standard models for the kinematics of the gas in the acceleration region of the circumstellar envelope fail to explain the observations. Pulsation of the gas associated to the star activity, rotation, and asymmetric mass loss processes are the most plausible processes involved in the formation of SiO line wings. Unfortunately, our limited angular resolution precludes a definitive answer to the origin of these wings.

A monitoring of the observed stars seems necessary to follow the variation of the SiO maser line wings as a function of the stellar phase. Such a monitoring has been started with the 30-m IRAM telescope and the results will be published elsewhere.

Sensitive VLBI, VLBA or VLA observations are needed to find the exact spatial extent and position of the blue and red wings observed in the maser emission of SiO in O-rich evolved stars.

Acknowledgements. We thank V. Bujarrabal and D. Downes for useful comments and suggestions. This work has been partly supported by the Spanish DGICYT under grant PB93-48. A.B. acknowledges support from the CNRS URA No. 352. J.C. acknowledges the Bordeaux University for a temporary professorship at the Bordeaux Observatory during the completion of this work

References

Barbier M., Mayor M., Mennessier O., Petit H. 1988, A&A Suppl., 72, 463
Baudry A. 1993, in The Structure and Content of Molecular Clouds, Springer Verlag, eds. T.L. Wilson & K.J. Johnston, in press
Bieniek R.J., and Green S., 1983, ApJ, 265, L29 (erratum: 270, L101)
Bowen G.H., 1988, ApJ 329, 299
Bowers P.F., Johnston K.J., De Vegt C. 1989, ApJ, 340, 479
Bowers P.F. 1991, ApJSS, 76, 1099
Bowers P.F., Johnston K.J. 1994, ApJSS, 92, 189
Bujarrabal V., 1994, A&A, 285, 953
Cernicharo J., Bujarrabal V., Lucas R. 1991, A&A, 249, L27
Cernicharo J., Bujarrabal V. 1992, ApJ, 401, L109
Cernicharo J., Bujarrabal V., Santarén J.L. 1993, ApJ, 407, L53
Cernicharo J., Brunswig W., Paubert G., Liechti S. 1994, ApJ, 423, L143
Danchi W.C., Bester M., DeGiacomi C.G. et al 1994, AJ, 107, 1469
Gómez Y., Rodríguez L.F., Contreras M.E., Moran J.M. 1994, Rev. Mexi. Astron., 28, 97
Diamond P., Kemball A.J., Benson J. et al. 1994, ApJ, 430, L61
González-Alfonso E.:1995, Ph.D. University of Valencia, Spain
Greenhill L.J., Colomer F., Moran J.M. et al 1995, ApJ, 449, 365
Hannif C.A., Ghez A.M., Gorham P.W. et al 1992, AJ, 103, 1662 Hinkle K.H., 1978 ApJ, 220, 210
Huggins P.J., Healy A.P., 1986 ApJ, 304, 418
Jewell P.R., Snyder L.E., Walmsley C.M., Wilson T.L., Gensheimer P.D. 1991, A&A, 242, 211
Kwok S. 1975, ApJ, 198, 583
Karovska M., Nisenson P., Papaliolios C., Boyle R.P. 1991, ApJ, 374, L51
Lockett P., Elitzur M., 1992, ApJ, 399, 704
Loup C., Forveille T., Omont A., Paul J.F.:1993, A&AS, 99, 231
Miyoshi M., Matsumoto K., Kameno S., et al. 1994, Nature, 371, 395
Morris M. 1987, PASP 99, 1115
Morris M. 1990, in From Miras to Planetary Nebulae, Editions Frontires, eds. M.O. Mennessier & A. Omont
Nyman L.A., Olofsson H., 1986, A&A, 158, 67
Planesas P., Bachiller R., Martín-Pintado J., Bujarrabal V. 1990 ApJ, 351, 263
Planesas P., Kenney J.D.P., Bachiller R. 1990, ApJ, 364, L9
Reid M.J., Menten K.M. 1990, ApJ, 360, L51
van der Veen W.E.C., Habing H.J. 1988, A&A, 194, 125
van Blerkom D.V. 1978, ApJ, 223, 835
van Blerkom D.V., Auer L. 1976, ApJ, 204, 775
Wright M.C.H., Carlstrom J.E., Plambeck R.L, Welch W.J. 1990, AJ, 99, 1299
Zhou Zhen-pu, Kaifu N. 1984, A&A, 138, 359

This article was processed by the author using Springer-Verlag LaTeX A&A style file *L-AA* version 3.